

A Study of confinement for $Q\bar{Q}$ potentials on D3, M2 & M5 branes

Edward Quijada and Henrique Boschi-Filho

*Instituto de Física, Universidade Federal de Rio de Janeiro,
Caixa Postal 68528, RJ 21941-972, Brazil*

E-mail: edward@if.ufrj.br, boschi@if.ufrj.br

ABSTRACT: We study analytically and numerically the interaction potentials between a pair of quark and anti-quark on D3, M2 and M5 branes. These potentials are obtained using Maldacena's method involving Wilson loops and present confining and non-confining behaviours in different situations that we explore in this work. In particular, at the near horizon geometry the potentials are non-confining in agreement with conformal field theory expectations. On the other side, far from horizon, the dual field theories are no longer conformal and the potentials present confinement. This is in agreement with the behaviour of strings in flat space where the string mimics the expected flux tube of QCD. A study of the transition between the confining/non-confining regimes in the three different scenarios (D3, M2, M5) is also performed.

Contents

1	Introduction	1
2	Wilson loops in D3- M2- and M5-brane spaces	3
3	D3-brane	5
3.1	Non-confining behaviour	5
3.2	Confining behaviour	6
3.3	Deconfinement/Confinement transition	8
4	M2-brane	9
4.1	Non-confining behaviour	10
4.2	Confining behaviour	11
4.3	Deconfinement/Confinement transition	12
5	M5-brane	13
5.1	Non-confining behaviour	14
5.2	Confining behaviour	15
5.3	Deconfinement/Confinement transition	15
6	Conclusions	18

1 Introduction

Usually, in quantum field theory, the Wilson loop operator is defined as

$$W(C) = \frac{1}{N} \text{Tr} P e^{i \oint_C A},$$

where C denotes a closed loop in space-time and the trace is over the fundamental representation of the gauge field A with $SU(N)$ symmetry. In the particular case of a rectangular loop (of sides T and L), it is possible to calculate (in the limit $T \rightarrow \infty$) the expectation value for the Wilson loop:

$$\langle W(C) \rangle = \mathcal{A}(L) e^{-TE(L)},$$

where $E(L)$ can be identified with the energy of the quark-antiquark pair in the static limit.

Soon after the conjecture about the duality between M/string theory in AdS spaces and conformal gauge field theories [1–5], Maldacena [6], Rey and Yee [7] (MRY), proposed a method to calculate expectation values of the Wilson loop for the large N limit of field theories. This limit is calculated from a string theory in a given background using the gauge/gravity duality.

In this method, the expectation value of the Wilson loop is related to the worldsheet area S of a string whose boundary is the loop in question such that

$$\langle W(C) \rangle \sim e^S.$$

Maldacena used this approach to calculate the quark-antiquark potential for the string in the $AdS_5 \times S^5$ background [6] obtaining a non-confining potential for the infinitely massive quark-antiquark pair, consistent with the conformal symmetry of the dual super Yang-Mills theory. In other backgrounds the quark-antiquark potential can be confining as shown for instance in [8], where a confinement criterion was obtained.

This approach can also be extended to the finite temperature case [9, 10] by considering an AdS Schwarzschild background. In this case, the temperature of the conformal dual theory is identified with the Hawking temperature of the black hole [11]. This situation also leads to a non-confining potential for the quark-antiquark interaction.

The thermodynamic of D-brane probes in a black hole background were treated in [12]. These systems are holographically dual to a small number of flavours in a finite-temperature gauge theory. First order phase transitions were found characterised by a confinement/deconfinement transition of quarks.

A phenomenological approach was also considered calculating the Wilson loop for the string in some holographic AdS/QCD models. For instance, the hard-wall model exhibits a confining behaviour [13, 14] reproducing the Cornell potential. At finite temperature, this calculation gives a second order phase transition describing qualitatively a confinement/deconfinement phase transition [15]. Then, it was shown that a Hawking-Page phase transition [16] should occur for the hard- and soft-wall models at finite temperature [17–21]. In particular, for the soft-wall model, an interesting estimate of the deconfinement temperature was found [18], compatible with QCD expectations.

In a recent paper it were studied some geometric configurations of a static string on a D3-brane background [22] and also a string-like object on M2- and M5-brane backgrounds [23]. These geometric configurations corresponds to a gauge theory which describes the quark-antiquark interaction on the branes. For some specific geodesic regimes we found confining interactions and for others non-confining potentials were found.

In this paper we perform a systematic analytical and numerical study of the quark-antiquark potentials in D3- M2- and M5- brane backgrounds analysing their confining/non-confining behaviours in different situations, always at zero temperature. In particular, at the near horizon geometry the potentials are non-confining in agreement with conformal field theory expectations. On the other side, far from horizon, the dual field theories are no longer conformal and the potentials present confinement. This is in agreement with the expected behaviour of strings in flat space where the string mimics the flux tube model of QCD. In the cases of M2 and M5 branes in M-theory we choose a cigar-shaped membrane background such that that stringy picture of the dual flux tube also holds. We also focus in searching for the point in the geodesics at which the zero temperature confinement/deconfinement transition takes place.

2 Wilson loops in D3- M2- and M5-brane spaces

We start this study by considering the Wilson loop on the background generated by a large number of coincident D3-branes in string theory in 10 dimensional spacetime. The Nambu-Goto string action [24]:

$$S = \frac{1}{2\pi} \int d\sigma d\tau \sqrt{\det(g_{NM} \partial_\alpha X^N \partial_\beta X^M)} \quad (2.1)$$

is employed on this background, where the scale was set to $\alpha' = 1$, $X^N(\sigma, \tau)$ are the coordinates of the string worldsheet and g_{NM} is the background metric. The specific form of the metric is given in the next section. It is considered that the pair of quark-antiquark is contained in the D3-brane world which are attached to the ends of the open string that lives in 10 dimensions. For simplicity, we work in a static string configuration, that is represented in figure 1. The Wilson loop corresponds to a rectangle with sides L and T , where T is some time interval. This rectangle is associated with the worldsheet surface as shown in figure 2.

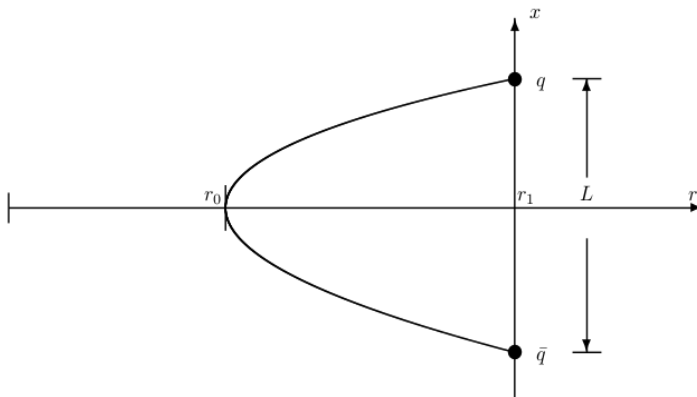


Figure 1. Position of quark q and anti-quark \bar{q} on the D3-brane (represented here by the x -axis) together with the static string as the curve which connects q and \bar{q} through r_0 .

Thus the distance separation L between the quark-antiquark pair may be computed starting from the geodesic of the static string on this D3-brane background. This distance turns out to be an expression in terms of r_0 and r_1 (respectively, minimum and maximum for r coordinate in the worldsheet. See [8, 22]):

$$L = 2 \int \frac{g(r)}{f(r)} \frac{f(r_0)}{\sqrt{f^2(r) - f^2(r_0)}} dr, \quad (2.2)$$

where

$$\begin{aligned} f^2(r) &= (2\pi)^{-2} g_{00}(r) g_{ii}(r), \\ g^2(r) &= (2\pi)^{-2} g_{00}(r) g_{rr}(r). \end{aligned}$$

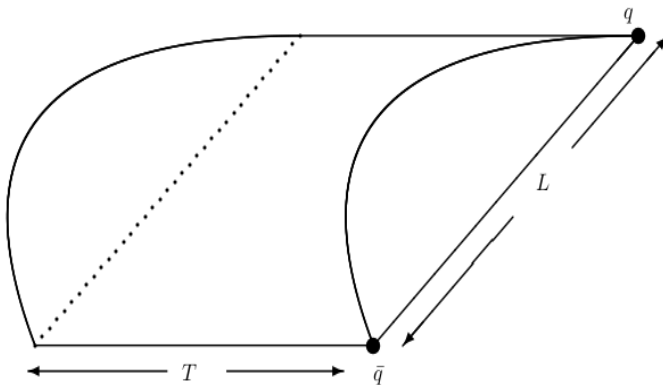


Figure 2. Curved worldsheet surface of the static string corresponding to a time interval T . The associated Wilson loop is the plane rectangle of sides T and L .

According to the MRY proposal the worldsheet area (S) is proportional to the energy interaction (V) between the quark-antiquark pair, so it may also be written down in terms of r_0 and r_1 :

$$V = 2 \int_{r_0}^{r_1} \frac{g(r)f(r)}{\sqrt{f^2(r) - f^2(r_0)}} dr - 2m_q. \quad (2.3)$$

Note that it is in general necessary to subtract the masses of the quarks m_q in order to obtain a finite result for the energy interaction.

We continue our study analysing the cases concerning M2- and M5-brane backgrounds. Since these backgrounds of 11-dimensional SUGRA corresponds to M-theory objects, it is not possible to start from Nambu-Goto action. Instead we should start from a 11-dimensional membrane action in those backgrounds [24, 25]:

$$S = \frac{1}{(2\pi)^2 l_{11}^3} \int d^3\sigma \left(\frac{(-\gamma)^{1/2}}{2} [\gamma^{ij} \partial_i X^M \partial_j X^N G_{MN}(X) - 1] + \epsilon^{ijk} \partial_i X^M \partial_j X^N \partial_k X^P A_{MNP}(X) \right), \quad (2.4)$$

where $i, j = 0, 1, 2$ are world-volume indices with γ^{ij} as the induced metric, $M, N, P = 0, \dots, 10$ are space-time indices with G_{NM} as the space-time metric, $X^N(\sigma^0, \sigma^1, \sigma^2)$ are the membrane coordinates, A_{MNP} is a three-form field with strength $F = dA$ and l_{11} sets the scale for the membrane (see [25]). After compactification of one spatial dimension of the membrane wrapped along the 11-th dimension of space-time we are able to reduce the membrane in 11 dimensions to a string-like object in 10 dimensions (see [26]). As a result we are able to work with string-like objects and similarly to the case of strings on D3 backgrounds, we utilize the static configuration and the MRY proposal to get the distance separation and energy interaction between a pair of quark-antiquark on M2-(M5)-branes (see [23]).

3 D3-brane

The solitonic solution of 10-dimensional supergravity that we are going to study is a space geometry generated by N coincident D3-branes. This solution is usually written down as [2, 27]:

$$ds^2 = \left(1 + \frac{R^4}{r^4}\right)^{-1/2} (-dt^2 + dx_3^2) + \left(1 + \frac{R^4}{r^4}\right)^{1/2} (dr^2 + r^2 d\Omega_5^2), \quad (3.1)$$

where R is a constant defined by $R^4 = 4\pi g N l_s^4$.

Following the MRY approach, the calculation of the distance separation L , Eq. (2.2), and the static potential interaction V , Eq. (2.3), between a pair of quarks on the D3-brane were obtained in [22]:

$$L = \frac{2r_0^3}{R^2} I_1\left(\frac{r_1}{r_0}\right) + \frac{2R^2}{r_0} I_2\left(\frac{r_1}{r_0}\right), \quad (3.2)$$

$$V = \frac{2r_0 \sqrt{r_0^4 + R^4}}{2\pi R^2 l_s^2} I_1\left(\frac{r_1}{r_0}\right) - 2m_q, \quad (3.3)$$

where

$$I_1\left(\frac{r_1}{r_0}\right) = \int_1^{r_1/r_0} dy \frac{y^2}{\sqrt{y^4 - 1}}, \quad (3.4)$$

$$I_2\left(\frac{r_1}{r_0}\right) = \int_1^{r_1/r_0} dy \frac{1}{y^2 \sqrt{y^4 - 1}}. \quad (3.5)$$

Following [8] we have that the quark mass must be:

$$2m_q = \frac{r_1}{\pi l_s^2}, \quad (3.6)$$

which diverges in the limit $r_1 \rightarrow \infty$.

In the following we are going to study the distance separation L , Eq. (3.2), and the potential energy V , Eq. (3.3), of the quark-antiquark pair in various different situations in the D3-brane solution.

3.1 Non-confining behaviour

Let us start our study considering the regime defined by $r_1 \gg r_0$ which means that the quark is very massive. Also we take $r_0 \ll R$ which means that we are in the near horizon geometry which corresponds approximately to the AdS₅ space. We take r_0 as the independent variable of parametrization with fixed R . Then, the behaviour of the distance separation L , Eq. (3.2), against r_0 is analysed. The numerical result is shown in figure 3, where we plot L/R vs. r_0/R . This plot shows a monotonic decreasing behaviour of L/R against r_0/R .

The next step is to analyse the behaviour of the potential V , Eq. (3.3), against the separation L , Eq. (3.2). The numerical result is shown in figure 4, where we plot V/R versus L/R . This plot shows an increasing function which goes to zero as L increases. So one can conclude that this plot corresponds to a non-confining potential which is essentially Coulomb like, as the one found by Maldacena in [6] for the case of the pure AdS space.

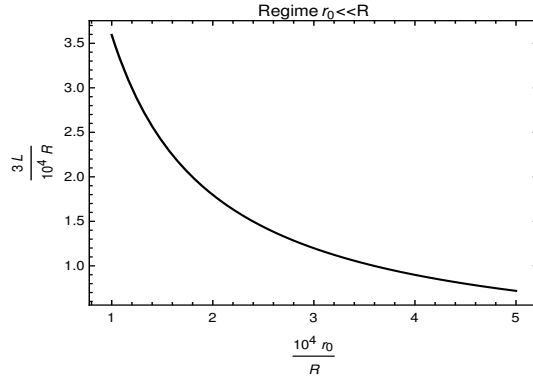


Figure 3. Monotonic decreasing behaviour of L/R vs. r_0/R . Here $r_1/R = 10^5$ and $r_0/R < 5 \times 10^{-4}$.

This result is also in agreement with [22] where a non-confining potential $V \sim -1/L$ was obtained in the regime $r_1 \gg r_0$ with $r_0 \ll R$. The dual field theory in this case is the well known $\mathcal{N}=4$ SYM which is a superconformal field theory. Then the non-confining behaviour found for the Wilson loop is in agreement with the conformal property of the dual theory.

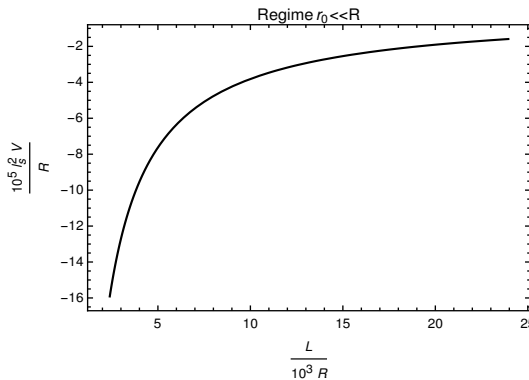


Figure 4. Non-confining potential interaction $l_s^2 V/R$ vs. L/R . Here $r_1/R = 10^5$ and $r_0/R < 5 \times 10^{-4}$.

3.2 Confining behaviour

Our next step is to analyse the regime $r_1 \gg r_0$ (very massive quark) but with $r_0 \gg R$ which corresponds to the region far from the horizon which is approximately a flat space geometry. First we perform a numerical study of the distance separation L , Eq. (3.2), against the minimum position of the string r_0 . The result of this analysis is presented in figure 5, where we plot L/R vs. r_0/R . This figure shows a monotonic increasing behaviour of L/R against r_0/R .

Then, the next step is to study the shape of the potential V , Eq. (3.3), against the separation distance L , Eq. (3.2). We did this numerical study and the result is presented in figure 6, where we plot the behaviour of V/R against L/R .

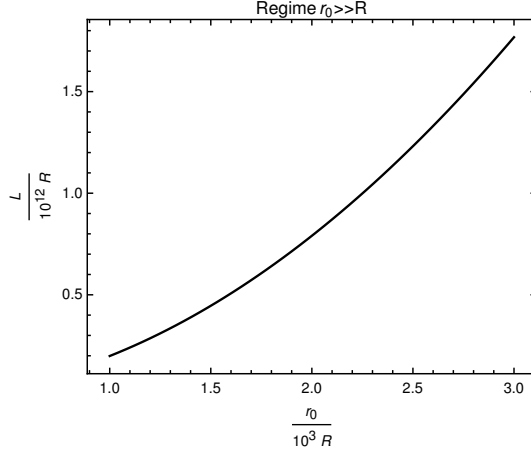


Figure 5. Increasing behaviour of L/R vs. r_0/R . Here $r_1/R = 10^5$ and $r_0/R > 10^3$.

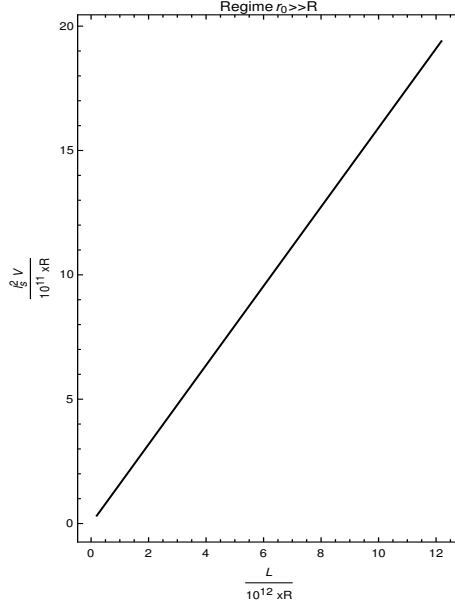


Figure 6. Plot of V/R vs. L/R with $r_1/R = 10^5$ and $r_0/R > 10^3$ which shows a confining potential.

Looking at figure 6 we see an almost straight line with positive derivative indicating that this plot implies a confining potential. This result is in agreement with ref. [22], where a linear confining potential was obtained in this regime for the quark antiquark pair in D3-brane space. The dual theory in this case is no longer conformal, since we are far from the horizon. Here, we can understand this picture as a string in flat space which mimics the confining flux tube of QCD.

3.3 Deconfinement/Confinement transition

In previous sections we obtained confining and non-confining behaviours for the potential energy V , Eq. (3.3), against the separation distance L , Eq. (3.2), in D3-brane space for different regimes of r_0 compared with R . So, we expect that a transition should occur between the regimes $r_0 \gg R$ (far from the horizon) and $r_0 \ll R$ (near the horizon).

In this section we work with $r_1 \gg r_0$ for r_0 values in the regime $r_0 \sim R$ such that we may find some deconfinement/confinement transition. Note that this is not a thermal phase transition since we are working at zero temperature. Instead, the expected transition should be related to the geometry of the D3-brane space.

First we present in figure 7 a plot showing how L/R varies against r_0/R . This picture shows a minimum value of r_0 which we call r^* .

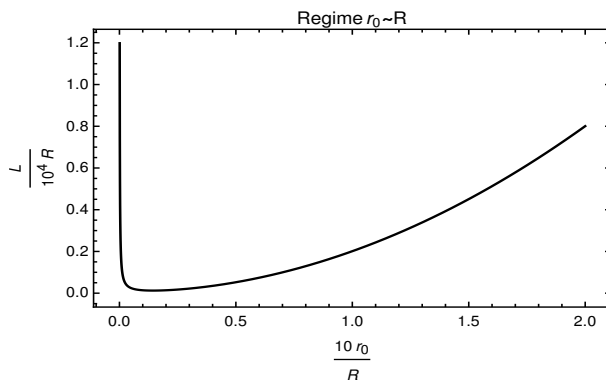


Figure 7. L/R vs. r_0/R . Here $r_1/R = 10^5$ and $r_0/R < 0.2$.

Note that it is also possible to define r^* from equations (3.2), (3.4) and (3.5). Using these equations we get an equation whose root is precisely r^* :

$$\frac{6r_*^2}{R^2} I_1\left(\frac{r_1}{r_*}\right) - \frac{2r_1^3}{R^2 r_* \sqrt{(r_1/r_*)^4 - 1}} - \frac{2R^2}{r_*^2} I_2\left(\frac{r_1}{r_*}\right) - \frac{2R^2}{r_1 r_* \sqrt{(r_1/r_*)^4 - 1}} = 0 \quad (3.7)$$

Some numerical solutions for this equation are shown in table 1.

Table 1. Some values of r^*/R in eq. (3.7) for different values of r_1/R .

r^*/R	r_1/R
9.87×10^{-3}	10^6
3.015×10^{-2}	10^5
6.687×10^{-2}	10^4
1.42×10^{-1}	10^3

The potential interaction V , Eq. (3.3), against the separation distance L , Eq. (3.2), in this regime is presented in figure 8. In this figure we can notice that there are two branches: the inferior one is a non-confining Coulomb-like potential, and the superior one is a confining potential that has a monotonic increasing behaviour as L/R is increased.

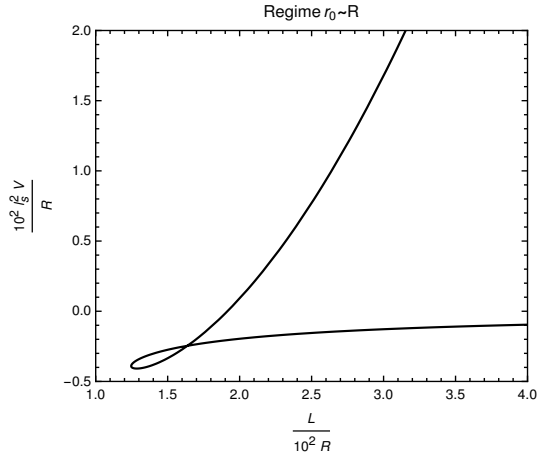


Figure 8. Transition of the potential interaction. Here $r_1/R = 10^5$.

From fig. 8, our analysis shows that the $r_0 < r^*$ condition corresponds to non-confining behaviour and $r_0 > r^*$ condition corresponds to confining one. This is the expected transition in the confinement/deconfinement behaviour of the quark-antiquark pair potential in D3-brane space. The transition seems to occur near the region $r_0 \sim r^*$. It is important to remark that this is not a thermal phase transition since we are working at zero temperature and the transition is of geometrical nature.

4 M2-brane

In the previous section, we presented an analysis of the Wilson loop for the D3-brane background. Here in this section and in the following we are going to present a similar discussion for other backgrounds such as M2- and M5-brane spaces. Although these background spaces belong to 11-dimensional M-theory that must correspond to higher dimensional objects like membranes, it is possible to do a dimensional reduction. This consists in compactifying one dimension of the membrane along one spacial direction, in order to have a string-like configuration in 10-dimensional background spaces. For details see [23, 26].

We start the study of confinement with the MRY method in SUGRA-backgrounds with the case of the space generated by N coincident M2-branes. The 11-dimensional supergravity M2-brane solution is given by the metric (see [4, 5, 25]):

$$ds_{\text{M2}}^2 = \left(1 + \frac{R_2^6}{r^6}\right)^{-2/3} dx_3^2 + \left(1 + \frac{R_2^6}{r^6}\right)^{1/3} (dr^2 + r^2 d\Omega_7^2), \quad (4.1)$$

where R_2 is a constant defined by $R_2 = (32\pi N l_{11}^6)^{1/6}$, N is the number of coincident branes, l_{11} is the Plank's length in eleven dimensions and $d\Omega_7$ is the differential solid angle for seven-sphere.

In a previous work [23] the distance separation (L) and static potential (V) for a pair of quarks in a M2-brane space were obtained:

$$L = 2r_0 \int_1^{r_1/r_0} dy \frac{\left(1 + \frac{\epsilon}{y^6}\right) y^3}{\sqrt{y^8 - y^6 + \epsilon(y^8 - 1)}}, \quad (4.2)$$

$$V = \frac{2r_0^2 \sqrt{1 + \epsilon}}{2\pi l_{11}^3} \int_1^{y_1} dy \frac{y^5}{\sqrt{y^8 - y^6 + \epsilon(y^8 - 1)}} - 2m_q, \quad (4.3)$$

where r_0 ($-r_1$) is the minimum(-maximum) value of coordinate r associated with the string-like object obtained by dimensional reduction and $\epsilon = (R_2/r_0)^6$. Again following ref. [8], we can compute the quark mass m_q as:

$$2m_q = \frac{r_1^2}{2\pi l_{11}^3}, \quad (4.4)$$

which diverges if we let $r_1 \rightarrow \infty$.

4.1 Non-confining behaviour

In this section we work in the geometric regime $r_0 \ll r_1$ which corresponds to very massive quarks and with $r_0 \ll R_2$ which means that we are in the near horizon geometry which is approximately AdS₄. First we plot in figure 9 the distance L/R_2 , eq. (4.2), against r_0/R_2 . We can notice from this plot that L has a monotonic decreasing behaviour as r_0 is increased.

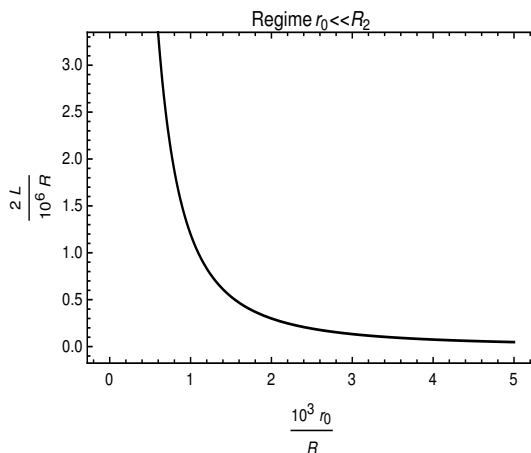


Figure 9. Distance L/R_2 between quarks in a M2-brane space vs. r_0/R_2 . Here $r_1/R_2 = 10^4$, $r_0/R_2 < 5 \times 10^{-3}$.

Next, we plot in figure 10 the potential interaction $l_{11}^3 V/R_2^2$, eq.(4.3), against the distance of the quark-antiquark pair L/R_2 , eq.(4.2). As we can note from this plot, the potential interaction in this case turns out to have a Coulomb-like non-confining behaviour. This is in agreement with the result obtained in this same regime in ref. [23] and with the fact that the dual field theory is conformal, since we are in the near horizon geometry which is approximately AdS₄.

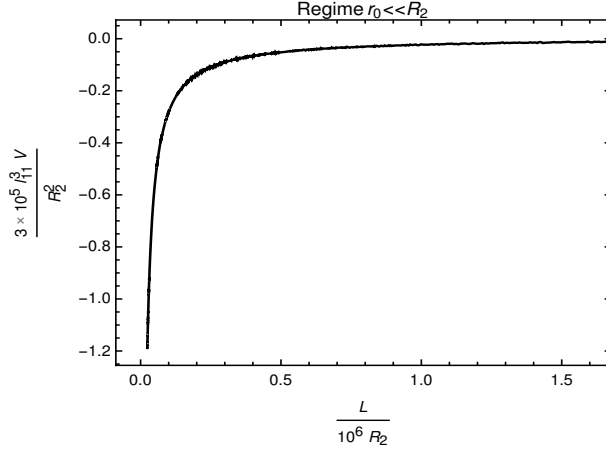


Figure 10. Potential $l_{11}^3 V/R_2^2$ between quarks in a M2-brane space vs. L/R_2 . Here $r_1/R_2 = 10^4$, $r_0/R_2 < 5 \times 10^{-3}$.

4.2 Confining behaviour

Here we still work in the regime $r_1 \gg r_0$, but with $r_0 \gg R_2$, which corresponds to the region far from the horizon which is approximately a flat space. Now we plot in figure 11 the rationalised distance L/R_2 , eq.(4.2), against r_0/R_2 . From this plot we can see that the distance L has an increasing behaviour as r_0 is increased. Notice that this behaviour is almost linear.

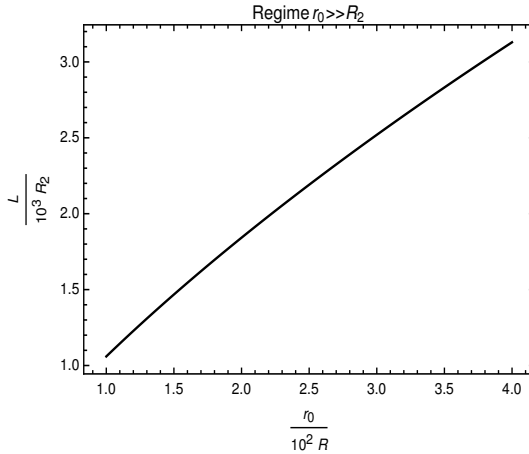


Figure 11. Distance L/R_2 between quarks in a M2-brane space vs. r_0/R_2 . Here $r_1/R = 10^4$ and $r_0/R_2 > 10^2$.

Next, continuing in the same geometric regime, we plot in figure 12 the potential $l_{11}^3 V/R_2^2$, eq.(4.3), against L/R_2 , eq.(4.2). We can see from this plot that potential interaction V has positive derivative, which means a confining behaviour. This behaviour is expected since we are working in the region far from the horizon of the M2-brane geometry where the dual field theory is non-conformal.

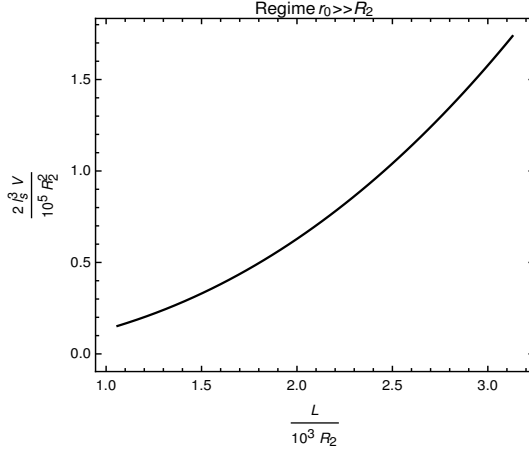


Figure 12. Potential $l_{11}^3 V/R^2$ between quarks in a M2-brane space vs. L/R_2 for $r_0 \gg R_2$. Here $r_1/R = 10^4$ and $r_0/R_2 > 10^2$.

4.3 Deconfinement/Confinement transition

In the last subsections we had a non-confining behaviour at the regime $r_0 \ll R_2$ and a confining one at $r_0 \gg R_2$. So in this section we look for a transition behaviour at a middle term regime $r_0 \sim R_2$.

First we plot the distance L/R_2 between quarks, eq.(4.2), against r_0/R_2 , which is shown in figure 13. From this plot we notice that there is a minimum at $r_0 = r^*$.

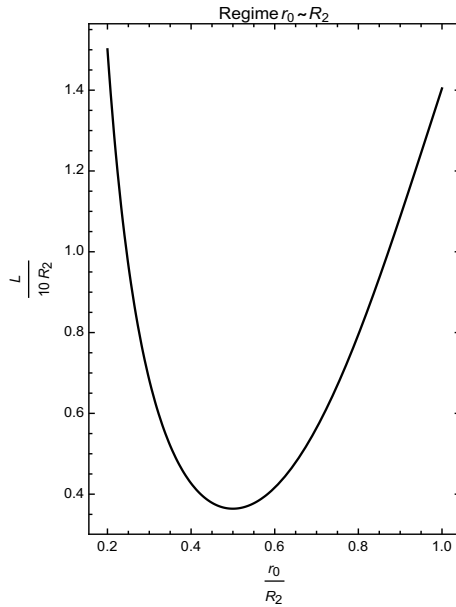


Figure 13. Distance L/R_2 between quarks in a M2-brane space vs. r_0/R_2 . Here $r_1/R_2 = 10^4$, $r_0/R \leq 1$ and $r^*/R = 0.500$.

Also we can get this value r^* as a root of an equation that can be derived from (4.2):

$$\frac{d}{dr_0} L(r_0/R_2) = 0. \quad (4.5)$$

Some solutions of this equation are presented on table 2 for different values of r_1/R_2 .

Table 2. Some values of r^*/R_2 in eq. (4.5) for different values of r_1/R_2 .

r^*/R_2	r_1/R_2
0.500	1×10^4
0.503	8×10^3
0.510	4×10^3
0.524	1×10^3

Next we plot in figure 14 the potential $l_{11}^3 V/R_2^2$, eq.(4.3), against the distance L/R_2 , eq.(4.2). We notice from this plot that there are two branches: the inferior one corresponding to a non-confining Coulomb-like potential and the superior one corresponding to a confining potential. Also, from our analysis of the last plots, we can conclude that for $r_0 < r^*$ the potential is a non-confining one while for $r_0 > r^*$ the potential is a confining one.

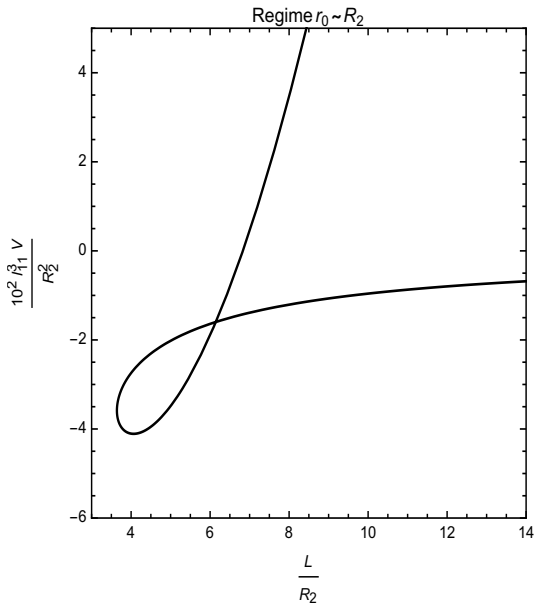


Figure 14. Potential $l_{11}^3 V/R_2^2$ between quarks in a M2-brane space vs L/R_2 .

5 M5-brane

Now we analyse the confinement behaviour of a quark-antiquark pair using the MRY method in the 11-dimensional SUGRA background space generated by N coincident M5-

branes. The metric solution is [4, 5]:

$$ds_{M5}^2 = \left(1 + \frac{R_5^3}{r^3}\right)^{-1/3} dx_6^2 + \left(1 + \frac{R_5^3}{r^3}\right)^{2/3} (dr^2 + r^2 d\Omega_4^2), \quad (5.1)$$

where R_5 is a constant given by $R_5 = (\pi N l_{11}^3)^{1/3}$.

According to [23], the distance separation and the potential interaction of a pair of quarks are given by:

$$L = 2r_0 \int_1^{r_1/r_0} dy \frac{(1 + \epsilon/y^3)^{1/2}}{(y^2 - 1)^{1/2}} \quad (5.2)$$

$$V = \frac{r_0^2}{\pi l_{11}^3} \int_1^{r_1/r_0} dy \frac{y^2 (1 + \epsilon/y^3)^{1/2}}{(y^2 - 1)^{1/2}} - 2m_q \quad (5.3)$$

where r_0 ($-r_1$) is the minimum(-maximum) value of coordinate r of the string-like object obtained from dimensional reduction and $\epsilon = R_5^3/r_0^3$. Following ref. [8] we can compute the quark mass:

$$2m_q = \frac{1}{\pi l_{11}^3} \int_0^{r_1} dr r \sqrt{1 + \left(\frac{R_5}{r}\right)^3}, \quad (5.4)$$

which is divergent in the limit $r_1 \rightarrow \infty$.

5.1 Non-confining behaviour

We work here in the regime $r_1 \gg r_0$ which means that the quarks are very massive and with $r_0 \ll R_5$ corresponding the region near horizon which in this case is approximately an AdS₇ geometry. For this regime the distance L/R_5 between the pair of quarks, eq.(5.2), against r_0/R_5 is plotted in figure 15. This plot shows that the distance L has a monotonic decreasing behaviour as r_0 is increased.

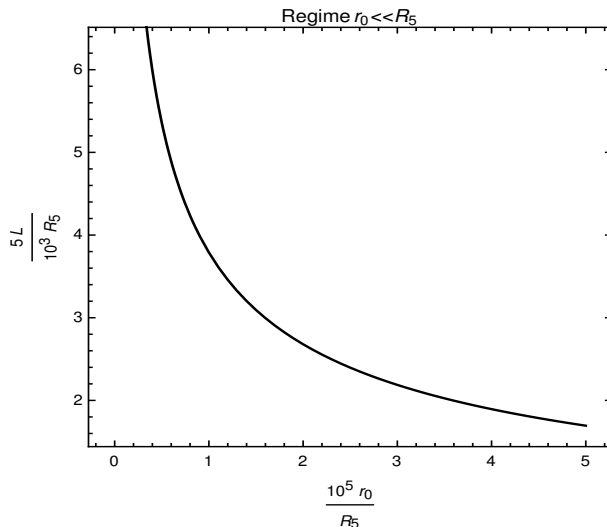


Figure 15. Distance L/R_5 between quarks vs. r_0/R_5 . Here $r_1/R_5 = 10^2$, $r_0/R_5 < 5 \times 10^{-5}$.

Next we plot in figure 16 the potential interaction $l_{11}^3 V/R_5^2$, eq.(5.3), against the distance separation between quarks L/R_5 , eq.(5.2). We can see from this plot that the potential V shows a non-confining behaviour: it has a negative slope and it goes to minus infinite as L increases. This is the expected behaviour since we are in the near horizon region where the metric is approximately an AdS₇ compatible with a conformal field theory.

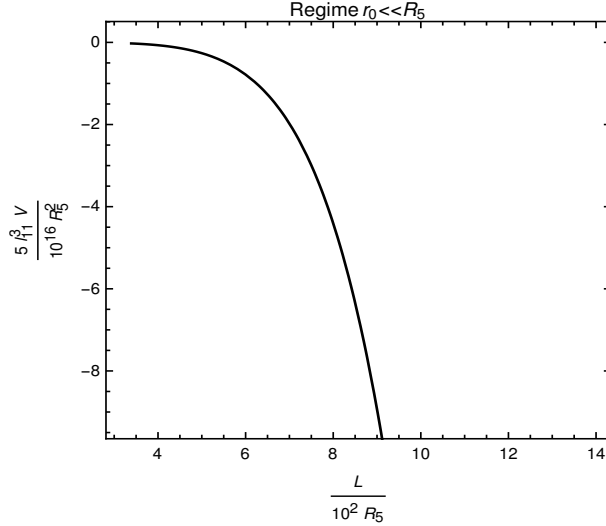


Figure 16. Potential $l_{11}^3 V/R_5^2$ between quarks in a M5-brane space vs. the distance L/R_5 . Here $r_1/R_5 = 10^2$ and $r_0/R_5 < 5 \times 10^{-5}$.

5.2 Confining behaviour

In this subsection we still work in the regime $r_1 \gg r_0$ but with $r_0 \gg R_5$ (far from the horizon) which corresponds to an approximately flat space geometry. In this regime we plot in figure 17 the distance separation L/R_5 , eq.(5.2), against r_0/R_5 . We can see from this plot that L shows an almost linear behaviour as r_0 is increasing.

Next we plot in figure 18 the potential interaction $l_{11}^3 V/R_5^2$ between the pair of quarks, eq.(5.3), against the distance between quarks L/R_5 , eq.(5.2). From this plot we can notice that the potential V shows a confining behaviour: it has a positive slope as L is increased. This behaviour is expected since we are working in the region far from the brane which approaches asymptotically a flat space so that the dual field theory is no longer conformal.

5.3 Deconfinement/Confinement transition

In the last subsections we found non-confining potential behaviour at $r_0 \ll R_5$ and confining potential behaviour at $r_0 \gg R_5$. In this section we work in the regime $r_0 \sim R_5$ and look for a confinement/deconfinement transition. First we plot in 19 the distance separation between quarks L/R_5 , eq.(5.2), against r_0/R_5 . From this plot we can notice that there is a minimum at the position $r_0 = r^*$.

We can also get r^* as a root of a equation that is obtained deriving equation (5.2):

$$\frac{d}{dr_0} L(r_0/R_5) = 0. \quad (5.5)$$

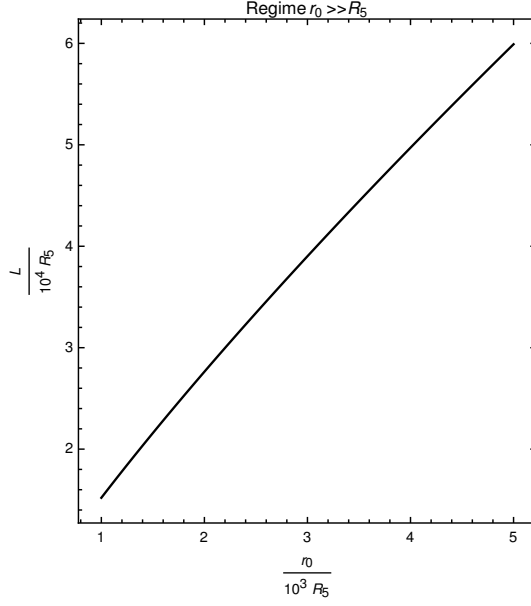


Figure 17. Distance L/R_5 between quarks in a M5-brane space vs. r_0/R_5 . Here $r_1/R_5 = 10^6$ and $r_0/R_5 > 10^3$.

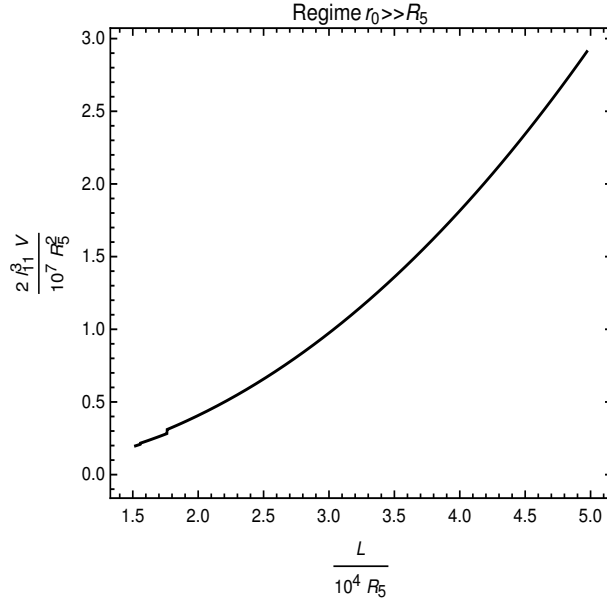


Figure 18. Potential interaction $l_{11}^3 V/R_5^2$ between quarks in a M5-brane space vs. the distance L/R_5 . Here $r_1/R_5 = 10^6$ and $r_0/R_5 > 10^3$.

Some solutions of this equation are shown in table 3 for some values of r_1/R_5 .

Finally we plot in figures 20 and 21 the potential interaction $l_{11}^3 V/R_5^2$, eq.(5.3), against the distance separation between quarks L/R_5 , eq.(5.2). From these plots we can see that we have two branches: The superior one in figure 20, which continuation for larger values of L/R_5 is amplified in figure 21, corresponds to a confining potential interaction, since we

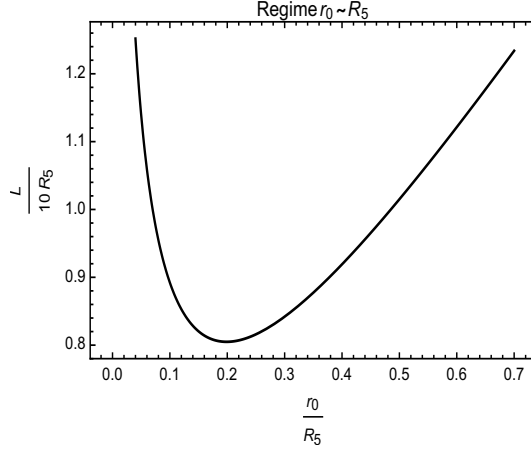


Figure 19. Distance L/R_5 between quarks in a M5-brane space vs. r_0/R_5 . Here $r_1/R_5 = 10^3$, $r_0/R_5 < 0.7$ and $r^*/R_5 = 0.19$.

Table 3. Some values of r^*/R_5 in eq. (5.5) for different values of r_1/R_5 .

r^*/R_5	r_1/R_5
0.19	1×10^3
0.21	5×10^2
0.25	1×10^2
0.42	1×10^1

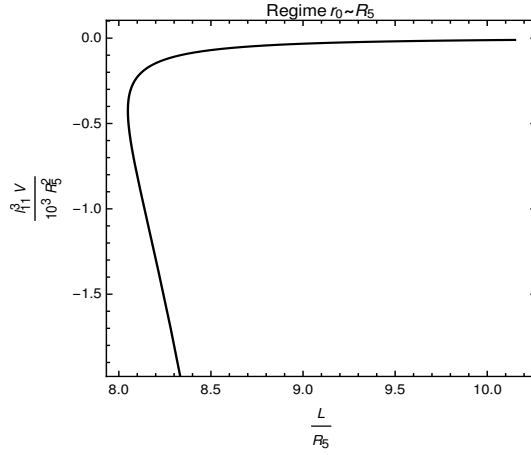


Figure 20. Potential interaction $l_{11}^3 V/R_5^2$ between quarks in a M5-brane space vs. L/R_5 . Here $r_1/R_5 = 10^3$, $r_0/R_5 < 0.5$ and $r^*/R_5 = 0.19$.

can observe that it has a positive derivative as L increases. On the other side, the inferior one, that is just presented in figure 20, corresponds to a non-confining potential.

Also we can conclude from these plots that values with $r_0 < r^*$ correspond to a non-confining behaviour, and values with $r_0 > r^*$ correspond to a confining behaviour.

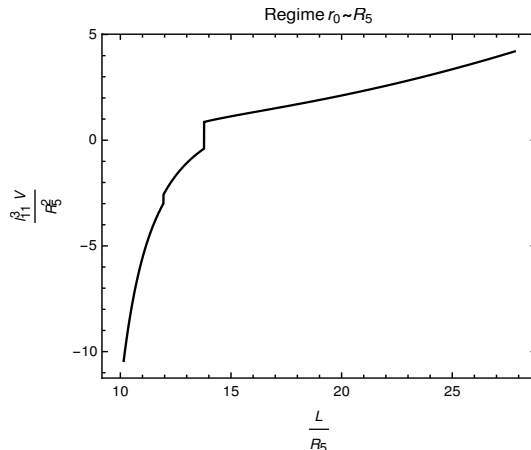


Figure 21. Potential interaction $l_{11}^3 V / R_5^2$ between quarks in a M5-brane space vs. L / R_5 . Here $r_1 / R_5 = 10^2$, $0.5 < r_0 / R_5$ and $r^* / R_5 = 0.19$.

6 Conclusions

We have analysed the Wilson loops for D3-, M2-, and M5-brane backgrounds using the MRY approach. As was discussed previously in refs. [22, 23] these backgrounds imply confining and non-confining quark-antiquark potentials depending on the geometric regime considered. We investigated here these situations further and mainly the transition between these two confinement behaviours.

In general for the three geometries that we have studied, we notice that as the distance separation L / R_i has a monotonic decreasing behaviour with r_0 , one finds a non-confining potential interaction. This situation occurs at the regime $r_1 \gg r_0$ and $r_0 \ll R_i$, which corresponds to heavy quark masses in AdS geometries (R_i assumes the values R , R_2 , and R_5 for the geometries D3-, M2-, and M5-branes, respectively).

On the other hand, when the distance separation L / R_i is a monotonic increasing function of r_0 , one finds a confining potential interaction. This situation occurs at the regime $r_1 \gg r_0$ and $r_0 \gg R_i$, which corresponds to heavy quark masses in flat space geometries. This confining behaviour can be understood looking at the metric in the region far from the brane. In this case the metric approaches a flat spacetime so that the dual field theory is no longer conformal. This situation is analogous to a string in flat space which mimics the flux tube model of QCD showing confinement.

We found out that the confinement/deconfinement transition occurs at a point r^* in the regime $r_0 \sim R_i$ for the D3, M2, and M5-brane backgrounds. The point r^* is where the non-monotonic L distance function of r_0 is a minimum. The value of r^* depends on r_1 and R_i and we have tabulated possible values in tables 1, 2 and 3, for each geometry. This situation occurs at the regime $r_1 \gg r_0$ (heavy quark) and corresponds to a transition between the AdS and flat space geometries. All these situations were analysed at zero temperature, so that the nature of the transitions are purely geometrical and not thermodynamical.

It would be interesting to analyse if this discussion can be extended to other Wilson loop configurations where $1/N$ corrections are present [28–31].

Acknowledgments

We would like to thank C. Hoyos for interesting discussions at the *Strings at Dunes* conference in Natal, Brazil, 2016, where a previous version of this work was presented. We would like also to thank CNPq - Brazilian agency - for financial support.

References

- [1] J. M. Maldacena, “The Large N limit of superconformal field theories and supergravity,” *Int. J. Theor. Phys.* **38**, 1113 (1999) [*Adv. Theor. Math. Phys.* **2**, 231 (1998)] [hep-th/9711200].
- [2] S. S. Gubser, I. R. Klebanov and A. M. Polyakov, “Gauge theory correlators from noncritical string theory,” *Phys. Lett. B* **428**, 105 (1998) [hep-th/9802109].
- [3] E. Witten, “Anti-de Sitter space and holography,” *Adv. Theor. Math. Phys.* **2**, 253 (1998) [hep-th/9802150].
- [4] O. Aharony, S. S. Gubser, J. M. Maldacena, H. Ooguri and Y. Oz, “Large N field theories, string theory and gravity,” *Phys. Rept.* **323**, 183 (2000) [hep-th/9905111].
- [5] J. L. Petersen, “Introduction to the Maldacena conjecture on AdS / CFT,” *Int. J. Mod. Phys. A* **14**, 3597 (1999) [hep-th/9902131].
- [6] J.M.Maldacena, “Wilson loops in Large-N field theories,” *Phys. Rev. Lett.* **80**(1998) 4859 [hep-th/9803002].
- [7] S. J. Rey and J. T. Yee, “Macroscopic strings as heavy quarks in large N gauge theory and anti-de Sitter supergravity,” *Eur. Phys. J. C* **22**, 379 (2001) [hep-th/9803001].
- [8] Y. Kinar, E. Schreiber and J. Sonnenschein, “Q anti-Q potential from strings in curved space-time: Classical results,” *Nucl. Phys. B* **566**, 103 (2000) [hep-th/9811192].
- [9] A. Brandhuber, N. Itzhaki, J. Sonnenschein and S. Yankielowicz, “Wilson loops in the large N limit at finite temperature,” *Phys. Lett. B* **434**, 36 (1998) [hep-th/9803137].
- [10] A.Brandhuber, N. Itzhaki, J.Sonnenschein and S. Yankielowicz “Wilson Loops, Confinement and Phase Transitions in Large N Gauge Theories from Supergravity,” *JHEP* **06** (1998) 001 [hep-th/9803263].
- [11] E. Witten, “Anti-de Sitter space, thermal phase transition, and confinement in gauge theories,” *Adv. Theor. Math. Phys.* **2**, 505 (1998) [hep-th/9803131].
- [12] D. Mateos, R. C. Myers and R. M. Thomson, “Thermodynamics of the brane,” *JHEP* **0705**, 067 (2007) doi:10.1088/1126-6708/2007/05/067 [hep-th/0701132].
- [13] H. Boschi-Filho, N. R. F. Braga and C. N. Ferreira, “Static strings in Randall-Sundrum scenarios and the quark anti-quark potential,” *Phys. Rev. D* **73**, 106006 (2006) [Erratum-ibid. *D* **74**, 089903 (2006)] [hep-th/0512295].
- [14] O. Andreev and V. I. Zakharov, “Heavy-quark potentials and AdS/QCD,” *Phys. Rev. D* **74**, 025023 (2006) [hep-ph/0604204].
- [15] H. Boschi-Filho, N. R. F. Braga and C. N. Ferreira, “Heavy quark potential at finite temperature from gauge/string duality,” *Phys. Rev. D* **74**, 086001 (2006) [hep-th/0607038].
- [16] S. W. Hawking and D. N. Page, “Thermodynamics of Black Holes in anti-De Sitter Space,” *Commun. Math. Phys.* **87**, 577 (1983).

- [17] O. Andreev and V. I. Zakharov, “The Spatial String Tension, Thermal Phase Transition, and AdS/QCD,” *Phys. Lett. B* **645**, 437 (2007) [hep-ph/0607026].
- [18] C. P. Herzog, “A Holographic Prediction of the Deconfinement Temperature,” *Phys. Rev. Lett.* **98**, 091601 (2007) [hep-th/0608151].
- [19] K. Kajantie, T. Tahkokallio and J. T. Yee, “Thermodynamics of AdS/QCD,” *JHEP* **0701**, 019 (2007) [hep-ph/0609254].
- [20] O. Andreev and V. I. Zakharov, “On Heavy-Quark Free Energies, Entropies, Polyakov Loop, and AdS/QCD,” *JHEP* **0704**, 100 (2007) [hep-ph/0611304].
- [21] C. A. Ballon Bayona, H. Boschi-Filho, N. R. F. Braga and L. A. Pando Zayas, “On a Holographic Model for Confinement/Deconfinement,” *Phys. Rev. D* **77**, 046002 (2008) [arXiv:0705.1529 [hep-th]].
- [22] H. Boschi-Filho and N. R. F. Braga, “Wilson loops for a quark anti-quark pair in D3-brane space,” *JHEP* **0503**, 051 (2005) [hep-th/0411135].
- [23] E. Quijada and H. Boschi-Filho, “Wilson loops on M2-branes and M5-branes,” *Phys. Rev. D* **92** (2015) 6, 066010 [arXiv:1503.05982 [hep-th]].
- [24] K. Becker, M. Becker and J. H. Schwarz, “String theory and M-theory: A modern introduction,” Cambridge University Press, 2007.
- [25] M. J. Duff and K. S. Stelle, “Multimembrane solutions of $D = 11$ supergravity,” *Phys. Lett. B* **253**, 113 (1991). doi:10.1016/0370-2693(91)91371-2
- [26] M.J.Duff, P.S.Howe,T.Inami and K.S.stelle, “Superstrings in $D=10$ from supermenbranes in $D=11$ ” *Phys. Lett.B* **191**(1987).
- [27] G. T. Horowitz and A. Strominger, “Black strings and P-branes,” *Nucl. Phys. B* **360** (1991) 197. doi:10.1016/0550-3213(91)90440-9
- [28] D. Farquet and J. Sparks, “Wilson loops on three-manifolds and their M2-brane duals,” *JHEP* **1412**, 173 (2014) [arXiv:1406.2493 [hep-th]].
- [29] J. Gomis and F. Passerini, “Holographic Wilson Loops,” *JHEP* **0608**, 074 (2006) [hep-th/0604007].
- [30] J. Gomis and F. Passerini, “Wilson Loops as D3-Branes,” *JHEP* **0701**, 097 (2007) [hep-th/0612022].
- [31] E. I. Buchbinder and A. A. Tseytlin, “ $1/N$ correction in the D3-brane description of a circular Wilson loop at strong coupling,” *Phys. Rev. D* **89**, no. 12, 126008 (2014) [arXiv:1404.4952 [hep-th]].